

See discussions, stats, and author profiles for this publication at:
<https://www.researchgate.net/publication/223381532>

Reactivity of $(\text{H}^+)(\text{e}^-)$ color centers at the MgO surface: Formation of O_2^- and N_2^- radical anions

ARTICLE in SURFACE SCIENCE · SEPTEMBER 2003

Impact Factor: 1.93 · DOI: 10.1016/S0039-6028(03)01000-8

CITATIONS

25

READS

35

4 AUTHORS, INCLUDING:



Gianfranco Pacchioni

Università degli Studi di Milano-Bicocca

516 PUBLICATIONS 18,373 CITATIONS

SEE PROFILE



Peter V Sushko

University College London

129 PUBLICATIONS 2,984 CITATIONS

SEE PROFILE



Alexander L Shluger

University College London

363 PUBLICATIONS 8,967 CITATIONS

SEE PROFILE

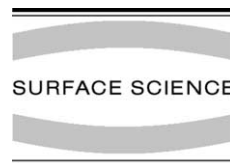


ELSEVIER

Available online at www.sciencedirect.com

SCIENCE @ DIRECT®

Surface Science 542 (2003) 293–306



www.elsevier.com/locate/susc

Reactivity of $(\text{H}^+)(\text{e}^-)$ color centers at the MgO surface: formation of O_2^- and N_2^- radical anions

Davide Ricci ^a, Gianfranco Pacchioni ^{a,*}, Peter V. Sushko ^b,
Alexander L. Shluger ^b

^a *Dipartimento di Scienza dei Materiali, Università di Milano-Bicocca, Istituto Nazionale per la Fisica della Materia, Via R. Cozzi 53, 20125 Milano, Italy*

^b *Department of Physics and Astronomy, University College London, Gower Street, London WC1E 6BT, UK*

Received 27 June 2003; accepted for publication 28 July 2003

Abstract

We have considered the interaction of O_2 and N_2 molecules with electrons trapped at the surface of MgO by performing embedded cluster DFT calculations. Trapped electrons at the surface of MgO react instantaneously with O_2 and N_2 leading to the formation of the corresponding O_2^- and N_2^- molecular anions stabilized at specific surface sites. So far, the atomistic model for this process was based on the idea that the electrons are trapped at oxygen vacancies, the F_s^+ centers. Recently, it has been shown that morphological sites at the MgO surface like a reverse corner, a step or a corner, can adsorb hydrogen and stabilize $(\text{H}^+)(\text{e}^-)$ pairs giving rise to a new class of paramagnetic color centers. Here we show that these centers exhibit reactivity towards O_2 and N_2 , which is fully consistent with the experimental observations, providing further support to the new model of electron traps at the MgO surface.

© 2003 Elsevier B.V. All rights reserved.

Keywords: Magnesium oxides; Surface chemical reaction; Magnetic phenomena (cyclotron resonance, phase transitions, etc.); Oxygen; Nitrogen molecule

1. Introduction

The nature of color centers at the MgO surface has been subject to a critical discussion in recent years [1–7]. These defect centers are interesting because their presence on as-grown materials does influence the chemical reactivity of the surface. For

example, the non-defective MgO[100] surface is totally inert towards O_2 and other molecular adsorbates [8,9] while a defective surface, prepared for instance by additive coloring experiments, is highly reactive and promotes the formation of stable superoxide anions, O_2^- [10]. The natural abundance of color centers in high surface area MgO samples prepared by thermal decomposition of $\text{Mg}(\text{OH})_2$ or MgCO_3 is too low to be monitored by standard spectroscopic techniques, like electron paramagnetic resonance (EPR) or UV–Vis. On the other hand, there is strong evidence that the surface contains several defective sites, mostly of

* Corresponding author. Tel.: +39-2-6448-5219; fax: +39-2-6448-6400.

E-mail address: gianfranco.pacchioni@unimib.it (G. Pacchioni).

morphological nature, that can act as precursor sites for the color centers, which are generated by electron trapping. Usually, the sample coloring is associated with the presence of oxygen vacancies, known as F centers, which in MgO can exist in three charged states: neutral F center (missing O atom), paramagnetic F^+ center (missing O^- ion), and F^{2+} center (missing O^{2-} ion).

Three main techniques are used to increase the number of color centers on polycrystalline MgO. One consists of the bombardment by X- or UV-rays, which generate electron–hole pairs [11,12]. Softer methods consist of the deposition of alkali metals, which transfer their valence electron to a pre-existing trapping site giving a paramagnetic center and an adsorbed cation [13–15]. Another chemical method is based on the adsorption of molecular hydrogen, which dissociates at some specific sites into a proton, H^+ (stabilized at O^{2-} anions) and a hydride, H^- (stabilized by surface cations) [1]. Under UV-irradiation the H^- species transforms into a neutral H atom and an electron trapped at a specific surface site. This leads to a characteristic EPR signal where the unpaired electron interacts strongly with some Mg cations of the surface but also exhibits a small interaction with a vicinal proton. These centers have been named $F_S(H^+)$ centers, based on the assumption that the electron is bound to a bare oxygen vacancy, the F^{2+} center, near an adsorbed proton [16].

The fact that the electrons generated with these methods populate surface (and not bulk or sub-surface) sites is shown by their interaction with probe molecules like O_2 , N_2 and CO [17–23]. In fact, these molecules react instantaneously with the surface color centers, with formation of stable (O_2^-) or metastable (CO^- , N_2^-) species. The reaction is accompanied by the complete disappearance of the color of the sample in the case of O_2 adsorption and its modification in the case of N_2 and CO. In both cases the characteristic EPR signal of the trapped electrons disappears. The entire process can be described by the following reaction:



In the past, all the features connected to reaction (1) have been explained using the classical model of the F_S^+ center, i.e. one electron trapped into an

oxygen vacancy at the [100] surface. This model was proposed by Tench and Nelson [24,25] more than 30 years ago as the obvious extension of the structure F centers in the bulk [26,27]. In recent years, a great effort has been done to better characterize the color centers at the surface of MgO, including their reactivity. Theoretical calculations show that the formation energy of the precursors of the color centers, the F_S^{2+} center, is very high; furthermore, their presence should be accompanied by negatively charged centers to maintain electroneutrality. Thus, the number of F_S^{2+} centers on the surface at thermal equilibrium is expected to be much smaller than that of the paramagnetic centers created by additive coloring.

New models have been proposed for the precursor sites of the paramagnetic color centers that do not belong to the category of oxygen vacancies [4,5,28,29]. These centers are usually classified as shallow electron traps and consist of neutral morphological defects (inverse kinks, low-coordinated cations, etc.) or even pairs of cation and anion vacancies. These precursors are neutral, i.e. do not alter the stoichiometry of the material, and the corresponding site becomes locally charged only after the electron trapping. Such sites can bind one electron by about 1–1.5 eV (shallow traps), and cannot account for the color of the sample, as their transition energies are too low.

Shallow traps can transform into deep electron traps by effect of the reaction with hydrogen [6,7] or alkali atoms [30]. The new centers consist of one of the morphological defects described above with an adsorbed proton or alkali metal cation; this is the case for instance of a reverse corner, MgO_{RC} , a shallow trap which transforms into a deep trap in the presence of an adsorbed proton, $MgO_{RC}(H^+)$ [6,7], or Na cation, $MgO_{RC}(Na^+)$ [30]. Similar effects are observed for other sites like cations at steps or corner, $MgO_{Step}(H^+)$ or $MgO_{Corner}(H^+)$. These centers are obtained by direct reaction with H_2 followed by UV light or by simple addition of alkali metals and they account much better than the traditional centers for a number of observations, like for instance the hyperfine interaction of the trapped electron with the surrounding and in particular with a proton, the color of the sample, its thermal stability, etc. This is most likely the actual

structure of what has been classified as $F_S(H)^+$ center in the past [1]. In this respect, the concept of oxygen vacancy is completely disappeared, and the symbol $F_S(H)^+$ has only an historical meaning (the new centers are in fact neutral, and a better name for them is $MgO_{site}(L^+)(e^-)$, where L stays for H or an alkali metal).

One aspect, which has still to be investigated in this context, is the reactivity of the new models of color centers towards gas-phase molecules, reaction (1). The reaction has been studied theoretically in detail for the “classical” F_S^+ and $F_S(H)^+$ centers [10,18,20,21]: the findings were in good agreement with the observations (in particular the energetics and the hyperfine interactions in the EPR spectra), thus reinforcing indirectly the validity of the classical model of color centers. Now, in the presence of a completely new model, we want to check if the reactivity towards O_2 and N_2 of an electron trapped at a reverse corner, at a step or at a corner site, $MgO_{site}(H^+)(e^-)$, is consistent with the observations, and to what extent it differs from that of the F_S^+ and $F_S(H)^+$ centers. The three sites considered are members of the family of morphological sites, which are precursors of paramagnetic color centers, and we expect that the conclusions derived on these centers are generally valid for the whole class of centers.

The paper has been organized as follows. In Section 2, we describe the cluster models and the theoretical methods used. Section 3 is divided in four parts. First we consider the interaction of O_2 with the “classical” F_S^+ center at the [1 0 0] terrace in order to compare the results with those reported in the literature. In the second part we present results for the reaction of O_2 and N_2 molecules with the new color centers. In the third part we compare the computed hyperfine coupling constants for the unpaired electron with the measured ones. The fourth part contains the summary of optical properties of the centers formed after reaction with O_2 and N_2 . The conclusions are summarized in the last section.

2. Details of calculations

For the calculations we employed an embedded cluster method [31] where the MgO surface is

represented by a large finite nano-cluster containing up to several thousands of atoms. The entire system is divided in two main regions. Region I is in the center of the cluster and contains the quantum-mechanical (QM) cluster surrounded by interface ions and by a region of classical shell model ions (polarizable). All centers in Region I are fully relaxed. Region II is represented by fixed rigid classical ions which correctly reproduce both the long-range (electrostatic potential) and the short-range interaction with atoms in Region I. The interface between the QM cluster and classical ions is needed in order to prevent the artificial spreading of the oxygen electron density outside the QM region; it consists of a semi-local effective core potential (ECP) [32] associated with the Mg^{2+} cations at the interface. The entire system, Region I plus Region II is neutral.

This hybrid scheme is implemented in the GUESS code [33] for the shell model part interfaced with the Gaussian98 code [34] for calculation of the QM cluster. The GUESS code allows one to calculate forces acting on all centers in Region I, both QM and classical (cores and shells), and simultaneously optimize their positions using the Broyden–Fletcher–Goldfarb–Shanno (BFGS) minimization technique [35]. The convergence of the method versus cluster size and shape has been analyzed in previous studies [5,6].

The total energy and the electronic structure of the QM cluster are calculated within the density functional theory (DFT) by solving the Kohn–Sham equations which include the matrix elements of the electrostatic potential due to all classical ions in Regions I and II, computed on the basis functions of the cluster. The gradient corrected Becke’s three parameters hybrid exchange functional [36], in combination with the correlation functional of Lee, Yang and Parr [37] (B3LYP) has been used for all the calculations.

To model the MgO surface we used a nano-cluster formed by $20 \times 20 \times 8$ centers, with the surface having a size of 20×20 atoms. A classical F_S^+ center is obtained from this nano-cluster by removing the central O atom in the first layer. The F_S^+ center at the [1 0 0] terrace was modeled using an $Mg_9O_{14}Mg_{21}^*$ QM cluster (Mg^* represents the interface Mg atoms).

A reverse corner site, formed at the intersection of two steps, has been obtained by removing a 5×5 ions fragment from the top layer of the $20 \times 20 \times 8$ array of ions, and was modeled using an $\text{Mg}_{17}\text{O}_{10}\text{Mg}_7^*$ QM cluster. The step was modeled by the same $20 \times 20 \times 8$ atoms nano-cluster with a half of the top layer removed and $\text{Mg}_{12}\text{O}_{13}\text{Mg}_{22}^*$ quantum cluster. A $20 \times 20 \times 20$ atoms nano-cluster and $\text{Mg}_{10}\text{O}_{13}\text{Mg}_{15}^*$ QM cluster were used to model an oxygen terminated corner site. In the next section we consider adsorption of O_2 and N_2 molecules on the same type of defect located at three different surface sites. These sites are defined as $\text{MgO}_{\text{RC}}(\text{H}^+)(\text{e}^-)$ for the reverse corner, $\text{MgO}_{\text{Step}}(\text{H}^+)(\text{e}^-)$ for the step, and $\text{MgO}_{\text{Corner}}(\text{H}^+)(\text{e}^-)$ for the oxygen-terminated corner.

The standard 6-31G basis set has been used for the Mg and O atoms of the QM cluster [38,39]. No basis functions were set on the interface atoms or in the vacancy when an atom is removed from the surface. This procedure produces similar results to those obtained by placing floating functions at the site where the electron is supposed to be trapped [21]. The 6-311 + G** basis set [40] has been used for the O_2 and N_2 molecules, and for the H atoms. The choice of the basis set for the N_2 molecule is a delicate problem due to the negative electron affinity (EA) of the molecule. With the 6-311 + G** basis set both the EA and the dissociation energy of N_2 are properly described: theoretical values of -1.61 eV for the EA and 9.75 eV for the D_e should be compared to the best estimate of the EA of -2.0 [41] and the experimental value for D_e of 9.80 eV [42]. The same is true for O_2 : theoretical values of EA = 0.43 eV and $D_e = 5.19$ eV compare well with the experimental values for EA = 0.45 eV and $D_e = 5.17$ eV [42]. All adsorption energies have been corrected by the basis set superposition error, BSSE, using the counterpoise correction [43]. The BSSEs for the systems studied are of the order of 0.2 – 0.3 eV.

Optimal geometry, binding energy (D_e), spin distribution, hyperfine coupling constants, and optical transitions have been determined and compared, when possible, with experimental data. The hyperfine interactions of the electron spin with the nuclear spin of the ^{14}N , ^{17}O , and ^1H nuclides

have been determined for the paramagnetic centers. The hyperfine spin-hamiltonian, $\mathbf{H}_{\text{hfc}} = \mathbf{S} \cdot \mathbf{A} \cdot \mathbf{I}$, is given in terms of the hyperfine matrix \mathbf{A} which describes the coupling between the electron and the nuclear spins [44]. The components of \mathbf{A} can be represented as the sum of an isotropic part, a_{iso} , related to the Fermi contact term, and the matrix \mathbf{B} which represents the “classical” dipolar interaction between two magnetic (electron and nuclear) moments. Typical anisotropic interactions can be observed when the unpaired electron is in directional orbitals like p, d, f, etc. The \mathbf{A} tensor can therefore be represented in matrix notation as $\mathbf{A} = a_{\text{iso}} + \mathbf{B}$.

3. Results and discussion

3.1. O_2 on F_S^+

Previous work has shown that the interaction between classical F_S^+ and $F_S(\text{H})^+$ centers (oxygen vacancies) with diatomic molecules like O_2 , CO, and N_2 leads to the formation of the corresponding molecular anions, X_2^- [10,18,20,21]. The reaction involves a crossing of electronic states as the molecule approaches the surface: the curve corresponding to the “neutral” interaction, dissociating into F_S^+ (or $F_S(\text{H})^+$) and X_2 units, is purely repulsive; at distances of about 2 Å, a crossing occurs between this state and a charge-transfer state, $F_S^{2+}-\text{X}_2^-$ (or $F_S(\text{H})^{2+}-\text{X}_2^-$); this latter state becomes the ground state for shorter distances and correlates at infinite distance with F_S^{2+} (or $F_S(\text{H})^{2+}$) and X_2^- charged fragments [20,21]. The observable properties of the process (energetics and hyperfine interactions) are quite consistent with the measurements. This finding has been used to corroborate the idea that the paramagnetic color centers present on the surface of MgO are oxygen vacancies with a single trapped electron [10,18,20,21]. So far, the calculations performed on this topic have been done using QM clusters embedded in point charges (PC) and the geometrical relaxation has been restricted to the small region of the QM cluster [10,18,20]. A first question to address is if the present method based on shell model embed-

ding provides results similar to those obtained in the previous studies [20,21].

Three possible orientations have been considered for the O_2 molecule approaching the surface [20,21]: two are parallel (A, B) and one is normal to the surface (C). In structure B the molecule is aligned along the $[100]$ direction connecting two Mg ions on the opposite site of the vacancy, while structure A, corresponding to the $[110]$ orientation, is tilted by 45° (Fig. 1). Only orientations A and C have been considered here. To model the F_S^+ center we used the $Mg_9O_{14}Mg_{21}^*$ QM cluster with a polarizable region of about 900 ions.

From the data of Table 1 one can see that essentially the same features have been obtained with PC- and shell-model (SM) embeddings. In particular, the adsorption energy, about 3.5 eV, is nearly

the same in the two sets of calculations. However, with the SM-embedding the symmetric orientation A is preferred by about 0.3 eV with respect to the normal orientation C, while with PC-embedding the two orientations are isoenergetic. The geometry of the adsorbed O_2 molecule, and the hyperfine interactions (not reported here) are very similar in the two cases. The strong interaction energy, computed with respect to F_S^+ and O_2 , is due to the formation of an O_2^- anion close to a F_S^{2+} site, giving rise to a strong electrostatic interaction.

Overall, the present theoretical method confirms the results obtained previously [20,21]. This allows us to directly compare results obtained on F_S^+ and $F_S(H^+)$ centers with those obtained here for the new class of $MgO(H^+)(e^-)$ paramagnetic color centers.

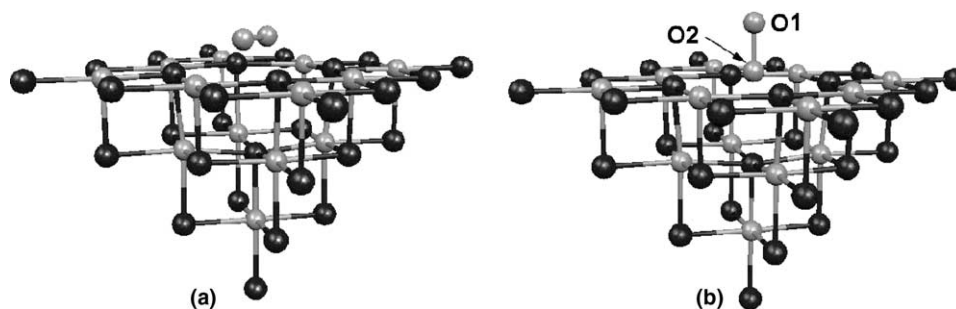


Fig. 1. Structure of the O_2/F_S^{2+} complex formed by interaction of the O_2 molecule with a surface oxygen vacancy, F_S^+ : (a) parallel orientation, see A in Table 1; (b) normal orientation, see C in Table 1. Black spheres: Mg; Gray spheres: O.

Table 1

Properties of O_2/F_S^+ surface complexes as obtained with embedding in point charges (PC-embedding) or in shell models (SM-embedding)

Model	O_2 orientation	D_e , eV	Spin density	a_{iso} , G	$d(O-O)$, Å	$z(O_2)^a$, Å
SM	A	3.66	O1 = 0.48 O2 = 0.48	O1 = 10.3 O2 = 10.3	1.33	0.968
PC ^b	A	3.43	O1 = 0.47 O2 = 0.47	O1 = 10.1 O2 = 10.1	1.33	0.966
SM	C	3.38	O1 = 0.28 O2 = 0.69	O1 = 8.0 O2 = 10.4	1.33	0.381
PC ^b	C	3.43	O1 = 0.26 O2 = 0.71	O1 = 7.6 O2 = 9.9	1.36	0.265

^a Vertical distance of the center of mass of the molecule from the surface.

^b Ref. [21]

3.2. O_2 and N_2 on $MgO(H^+)(e^-)$ surface centers

3.2.1. Reverse corner

We showed recently that a reverse corner, MgO_{RC} , can reversibly adsorb and dissociate H_2 at low temperature by means of ab initio calculations [6]. The resulting $MgO_{RC}(H^+)(H^-)$ center is diamagnetic and, upon UV-irradiation, transforms into a $MgO_{RC}(H^+)(e^-)$ neutral center by release of atomic hydrogen. The EPR signal of $MgO_{RC}(H^+)(e^-)$ is typical of paramagnetic color centers at the MgO surface, and most likely corresponds to what has been named the $F_S(H)^+$ center [6]. Similar $(H^+)(e^-)$ pairs form at other morphological sites like a step or a corner [7]. Also for the $MgO_{RC}(H^+)(e^-)$ center there are different possible structures, depending on the position of the proton which can be bound to a step O_{4c}^{2-} ion or to the five-coordinated O_{5c}^{2-} anion at the intersection of the two steps. This latter configuration is slightly less stable than the first one [6], but is more symmetric and is used here to check the reactivity towards O_2 and N_2 .

The reactivity of the $MgO_{RC}(H^+)(e^-)$ towards gas-phase molecules largely depends on properties like the energy required to remove the trapped electron from the color center (vertical ionization potential, IP) or, alternatively, the EA of the diamagnetic trap, $MgO_{RC}(H^+)$. Using the $Mg_{17}O_{10}Mg_7^*$ cluster, the EA of the $MgO_{RC}(H^+)$ center is 4.05 eV, i.e. 1.0 eV higher than that reported in our previous work (3.07 eV [6]); the difference

between old and new calculations is much smaller if we consider the vertical IP of the $MgO_{RC}(H^+)(e^-)$ center (5.07 versus 4.76 eV [6]). These differences are due to the use of a non-stoichiometric QM cluster. While this has almost no effect on most properties, it can result in some change when electrons are added to or removed from the system (see appendix in Ref. [6]). The use of non-stoichiometric clusters does partially affect the energetics of the charge transfer processes under investigation. In fact, we have considered the reaction of O_2 on F_S^+ (C orientation) using the nearly stoichiometric $Mg_{13}O_{14}Mg_{17}^*$ QM cluster and the non-stoichiometric $Mg_9O_{14}Mg_{21}^*$ one. The calculated interaction energies (not corrected for the BSSE) differ by 0.6 eV ($D_e = 3.0$ eV with $Mg_{13}O_{14}Mg_{17}^*$ and 3.6 eV with $Mg_9O_{14}Mg_{21}^*$). Thus, a large difference in EA reflects only partially in the D_e value. The reason is that in the surface complex the electron is not completely removed from the trapping site, as in a ionization process, but only partially displaced from the surface to the adsorbed X_2 molecule. The use of non-stoichiometric clusters however does not affect the qualitative conclusions of this study.

We found two possible orientations of the X_2 ($X = N, O$) molecule interacting with the $MgO_{RC}(H^+)(e^-)$ center (Fig. 2). Structure A has been found starting the geometry optimization with the X_2 molecule at about 1.5 Å from the top layer and the molecular axis oriented along the $[1\ 1\ 0]$ direction. Structure B has been obtained

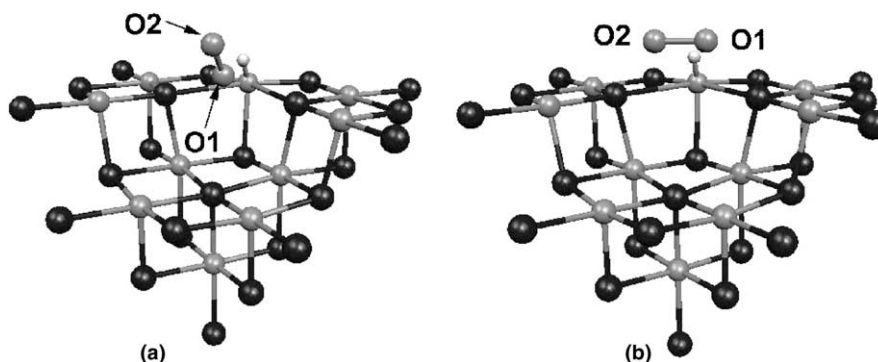


Fig. 2. Structure of the $O_2^-/MgO_{RC}(H^+)$ complex formed by interaction of the O_2 molecule with a surface neutral electron trap, $MgO_{RC}(H^+)(e^-)$, formed at a reverse corner: (a) “normal” orientation A in Table 2; (b) “parallel” orientation B in Table 2. A similar configuration is found for the N_2 molecule. Black spheres: Mg; Gray spheres: O.

Table 2

Properties of O₂ and N₂ molecules adsorbed on a MgO(H⁺)(e⁻) paramagnetic color center located at a reverse corner, at a step or at a corner of the MgO surface

		X ₂ orientation ^a	D _e , eV	Spin density	d(X–X), Å
Reverse corner	O ₂	A	2.93	O1 = 0.25 O2 = 0.73	1.35
		B	2.87	O1 = 0.50 O2 = 0.50	1.33
Step	O ₂	L	3.04	O1 = 0.37 O2 = 0.62	1.33
		U	2.53	O1 = 0.60 O2 = 0.40	1.34
Corner	O ₂	–	2.72	O1 = 0.50 O2 = 0.50	1.34
Reverse corner	N ₂	A	–0.07	N1 = 0.40 N2 = 0.54	1.18
		B	0.33	N1 = 0.46 N2 = 0.47	1.18
Step	N ₂	L	0.50	N1 = 0.33 N2 = 0.54	1.18
		U	–0.07	N1 = 0.46 N2 = 0.35	1.17
Corner	N ₂	–	0.17	N1 = 0.44 N2 = 0.44	1.18

^a A = parallel orientation; B = perpendicular orientation; L = lower terrace; U = upper terrace.

starting the optimization from the same initial point except that the molecular axis is tilted by 90° with respect to case A. At the end of the geometry optimization, in the orientation A the X₂ molecule maintains its alignment along the [1 1 0] direction, but is no longer parallel to the surface (Fig. 2). In fact, the molecule is rotated along the [1 0 0] direction with one atom near to the reverse corner (at ≈0.8 Å from the surface), and the second atom more distant. In the more symmetric orientation B the X₂ molecule maintains its axis normal to the [1 1 0] plane and is still parallel to the surface, with a distance from the closest surface ion of ≈1.6 Å (Table 2). As a consequence, the O or N atoms in the B orientation are equivalent by symmetry, at variance with structure A. The changes in the structure of the substrate induced by the presence of the adsorbate are minor.

3.2.2. Step

We found three possible configurations of the O₂ molecule at the step. One of them corresponds to the O₂ molecule being nearly upright above an

Mg ion at the upper terrace of the step. This configuration has a higher energy than the other two and, therefore, is excluded from further considerations.

The most stable configuration of the remaining two corresponds to the O₂ molecule adsorbed at the lower terrace of the step so that one of its atoms occupies a regular MgO lattice site and the other is pointing approximately along the step (conformation L in Table 2). The relaxed configuration is schematically shown in Fig. 3(a). For N₂ we found similar orientations, as reported in Table 2. For this configuration the spin density is unequally shared between the two oxygen atoms since their local atomic environment is very different. This can be attributed to the fact that one oxygen (O1) at the regular lattice site is coordinated by two lattice cations, while the other oxygen (O2) is closer to the H⁺ ion which contributes to the electrostatic potential at this site. Thus, the overall balance is in favor of the shared spin density.

In a search for a more symmetric configuration of the O₂ and N₂ molecules we considered X₂

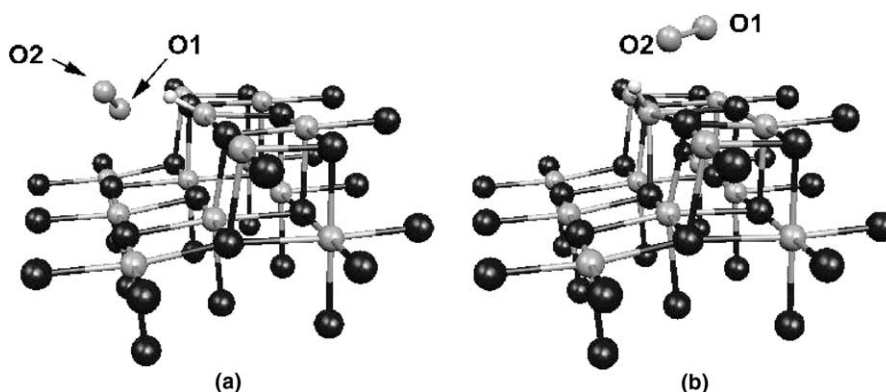


Fig. 3. Structure of the $\text{O}_2/\text{MgO}_{\text{Step}}(\text{H}^+)$ complex formed by interaction of the O_2 molecule with a surface neutral electron trap, $\text{MgO}_{\text{Step}}(\text{H}^+)(\text{e}^-)$, formed at a step: (a) lower terrace orientation; (b) upper terrace orientation. Similar configurations are found for the adsorbed N_2 molecule. Black spheres: Mg; Gray spheres: O.

adsorbed on the upper terrace of the step and oriented along $[1\ 1\ 0]$ near the H^+ ion (see configuration U in Table 2). This configuration is schematically shown in Fig. 3(b). It is clear that geometrically, the two atoms (O or N) of the X_2 molecule occupy similar sites. However, the corresponding spin densities are quite different. We believe that this is due to the difference in the electrostatic potential associated with the presence of the step.

3.2.3. Corner

Experiments report only one value for the isotropic hyperfine constant due to the interaction of the adsorbed oxygen with trapped electrons. This implies that the two oxygen or nitrogen atoms occupy positions that are symmetrical with respect to the adsorbed H. One of the possibilities is the $\text{MgO}_{\text{Corner}}(\text{H}^+)(\text{e}^-)$ defect where H is absorbed at the three-coordinated oxygen ion. We considered the adsorption of O_2 and N_2 on one of the three planes near the corner oxygen. It is clear from Fig. 4 that the resulting configuration is indeed symmetrical and both atoms of the adsorbed X_2 molecule share the same amount of the spin density (Table 2).

3.2.4. Electronic structure of O_2 and N_2 on $\text{MgO}(\text{H}^+)(\text{e}^-)$

The mechanism of the interaction of O_2 and N_2 with the $\text{MgO}(\text{H}^+)(\text{e}^-)$ site is the same for both

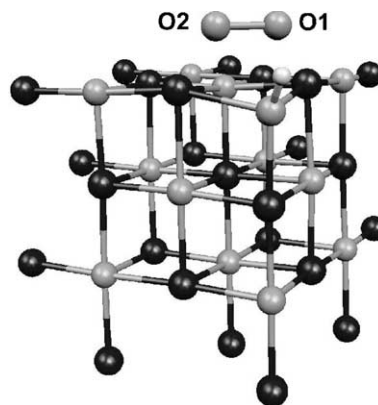


Fig. 4. Structure of the $\text{O}_2/\text{MgO}_{\text{Corner}}(\text{H}^+)$ complex formed by interaction of the O_2 molecule with a surface neutral electron trap, $\text{MgO}_{\text{Corner}}(\text{H}^+)(\text{e}^-)$, formed at a corner. Similar configuration is found for the adsorbed N_2 molecule. Black spheres: Mg; Gray spheres: O.

molecules and is independent of the site considered. It is also the same for F_s^+ and $\text{F}_s(\text{H}^+)$ centers [20,21]. In all cases there is a net charge transfer from the electron trap to the adsorbate when the molecule approaches the surface (Table 2). This is shown unambiguously by the computed properties. A first proof of the occurrence of the charge transfer comes from the analysis of the spin distribution. At large separations from the surface the spin is distributed in the MgO reverse corner. For short distances of O_2 and N_2 from the surface the

spin is entirely localized on the O or N atoms of the adsorbed molecule (Table 2). For the symmetric configurations of the adsorbed molecules, e.g. B orientation for the reverse corner in Fig. 2(b) and molecules at the corner site in Fig. 4, the spin distribution is symmetric, with 0.47 unpaired electrons per atom on N_2 and 0.50 electrons per atom in O_2 . For asymmetric configurations, e.g. A orientation for the RC site in Fig. 2(a) and molecules at the step in Fig. 3, the spin distribution is asymmetric, but the spin densities localized on N and O atoms add up to nearly exactly one unpaired electron on the O_2 or N_2 molecules. Another proof of the charge transfer is that the optimal O–O and N–N distances for the $MgO(H^+)(e^-)$ complexes are close to those calculated for the corresponding gas-phase molecular anions, X_2^- . In the following it is convenient to use notation $O_2^-/MgO(H^+)$ and $N_2^-/MgO(H^+)$ for the centers formed by adsorption of O_2 and N_2 respectively on surface $MgO(H^+)(e^-)$ color centers.

A graphic illustration of the charge transfer is provided by the plot of the spin density in the paramagnetic center before and after adsorbing a N_2 molecule (similar plots are obtained for O_2 but are not reported here for brevity). The plots show clearly that the electron trapped on a reverse corner is transferred to a π^* orbital on the N_2 adsorbate (Fig. 5).

3.2.5. Binding energies of $O_2^-/MgO(H^+)$ and $N_2^-/MgO(H^+)$ centers

The binding of O_2^- to the $MgO_{RC}(H^+)$ site is 2.93 eV for the A orientation and 2.87 eV for the B case (see Table 2). Thus, the two orientations are almost isoenergetic for O_2 . Adsorption energies of O_2 at the corner and step sites are close to those for the reverse corner and fall in the range of 2.5–3.0 eV. For the N_2^- complex at the reverse corner D_e is 0.33 eV for the symmetric orientation B, while structure A is slightly unbound, $D_e = -0.07$ eV. Again very similar energies are found for the N_2 at the $MgO_{Corner}(H^+)(e^-)$ and $MgO_{Step}(H^+)(e^-)$. The fact that the geometrical optimization does not lead to a spontaneous dissociation of N_2 is due to the presence of a small barrier in the potential energy surface.

The computed binding energies for $O_2^-/MgO(H^+)$ and $N_2^-/MgO(H^+)$ complexes are surprisingly similar to those found for the corresponding complexes formed at F_S^+ or $F_S(H^+)$ centers [20,21], despite the completely different geometric and electronic nature of the electron traps. Also for N_2 the present results are similar to those obtained on models of F_S^+ and $F_S(H^+)$ centers [20,21]. The results obtained on $MgO(H^+)(e^-)$ are also consistent with the experiments which show that while the O_2^- is a thermally stable complex [10], the N_2^- radical anion is metastable [17]. In fact, above 77 K the original signal of the

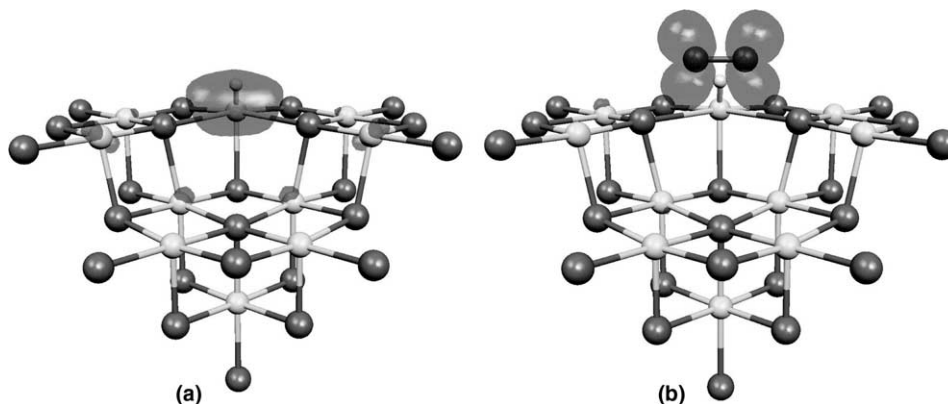


Fig. 5. Spin density plot for (a) $MgO_{RC}(H^+)(e^-)$ and (b) $N_2^-/MgO_{RC}(H^+)$. This shows the occurrence of a charge transfer from the surface to the adsorbed molecule.

trapped electron is restored as desorption of neutral N_2 occurs.

A simple cost–benefit analysis of the energy terms involved in the adsorption process on the example of the reverse corner provides a qualitative idea of the importance of the electrostatic interactions in reaction (1). In the following a positive energy indicates a cost and a negative energy indicates a gain. The cost to ionize the $MgO_{RC}(H^+)(e^-)$ is 5.07 eV. The addition of one electron to the free molecules leads to a gain of –0.43 eV for O_2 and to a cost of 1.61 eV for N_2 . Thus, the net cost for the charge transfer is 4.64 eV for O_2 and 6.68 eV for N_2 . The interaction energy is –2.93 eV for O_2 (bound) and +0.07 eV for N_2 (unbound); in both cases we refer to orientation A but of course the balance is similar for other orientations. Thus, the electrostatic interaction is 7.57 eV in the $O_2^-/MgO_{RC}(H^+)$ complex and 6.61 eV in the $N_2^-/MgO_{RC}(H^+)$ one. The larger electrostatic energy in the case of adsorbed oxygen is probably due to the fact that in this case the excess electron is more localized because of the higher EA of O_2 . The large energy difference between O_2 and N_2 , about 3 eV, arises in large part from the different EA's of the two molecules (≈ 2 eV), and to a smaller extent from the larger electrostatic interaction in the O_2 case (≈ 1 eV).

3.3. Hyperfine coupling constants

The analysis of the hyperfine coupling constants is very important because it allows a direct validation of the model by comparison with the experimental values. The isotropic and dipolar part of the hyperfine interaction, Table 3, have been computed for all the molecular ion complexes formed at the various sites considered. In general, they all show a close agreement with experiment for both O_2^- and N_2^- species. Furthermore, the properties of adsorbed O_2^- and N_2^- are virtually identical to those of the corresponding free molecular anions (Table 3). This provides an additional indication that the electronic structure of the O_2^- and N_2^- anions adsorbed on $MgO_{Site}(H^+)$ for the reverse corner, step and corner sites is almost identical to that of the free ions, consistent with the occurrence of the charge transfer.

EPR spectra obtained with ^{17}O -enriched O_2 and with N_2 molecules, respectively, on additively colored MgO have shown two main features: (a) the two nuclei of the molecule are magnetically equivalent, and (b) one component of the **A** tensor is much larger than the other two. This is what we found indeed for the “symmetric” orientations, like for instance orientation B of the reverse corner, or for the corner site. In this latter case the agreement is almost quantitative for both O_2^- and N_2^- species. However, the small energy difference between the various orientations and the variety of sites existing on the surface prevent a precise assignment. Furthermore, it is most likely that what is measured is a signal which is the superposition of similar signals arising from a variety of similar sites, thus resulting in an average situation.

The dependence of a_{iso} on the basis set was investigated for $O_2^-/MgO_{Corner}(H^+)$ center. We found that if the 6-311+G** basis set for the adsorbed oxygen atoms was fully uncontracted, the corresponding isotropic constants increase from 11.4 to about 14.3 G. These values would increase even further if instead of the B3LYP functional another one, with a larger contribution of the exact exchange, were used (e.g. HFLYP; this is due to the tendency of the HF exchange to produce strongly localized spin states). Thus, one has to keep in mind that the values of the hyperfine coupling constants, and in particular of the isotropic part, show some dependence on the details of the calculation.

3.4. Optical absorption of $O_2^-/MgO(H^+)$ and $N_2^-/MgO(H^+)$ centers

As we have mentioned before, the exposure of the MgO surface enriched with $F_S(H)^+$ centers to molecular oxygen results in a complete bleaching of the blue color due to these centers. An obvious test of the model then is to calculate the optical absorption properties of the complex formed after the absorption of O_2 on a surface color center. In the context of our model the complete bleaching shall mean that $O_2^-/MgO(H^+)$ centers have no optical absorption in the visible range. Similar test can be carried out for the $F_S(H)^+$ exposed to the

Table 3
Hyperfine coupling constants for the $X_2^-/\text{MgO}(\text{H}^+)$ complexes

	Orientation	Nucleus	a_{iso}	B_1	B_2	B_3
Free O_2^-			–10.8	29.1	30.4	–59.5
$\text{O}_2^-/\text{MgO}_{\text{RC}}(\text{H}^+)$	A	O1	–7.0	17.2	18.3	–35.5
		O2	–11.5	41.1	41.4	–82.6
		H	–1.2	–2.7	–1.9	4.6
	B	O1	–11.4	27.5	28.5	–56.0
		O2	–11.4	27.4	28.4	–55.8
		H	0.5	–3.1	–1.5	4.6
$\text{O}_2^-/\text{MgO}_{\text{Step}}(\text{H}^+)$	L	O1	–10.8	24.2	23.1	–47.3
		O2	–12.0	36.2	35.1	–71.3
		H	–0.5	–3.5	–3.0	6.4
	U	O1	–12.4	35.1	34.2	–69.3
		O2	–9.4	25.4	24.0	–49.3
		H	0.2	–3.1	–1.9	5.0
$\text{O}_2^-/\text{MgO}_{\text{Corner}}(\text{H}^+)$	–	O1	–11.4	30.4	29.3	–59.7
		O2	–11.4	30.4	29.3	–59.7
		H	0.0	–1.7	–1.3	3.0
O_2^-/MgO , exp. ^a		O	–20.3	27.5	28.6	–56.0
		H	0.1	–2.3	–1.4	3.8
Free N_2^-			2.1	–7.5	–8.0	15.6
$\text{N}_2^-/\text{MgO}_{\text{RC}}(\text{H}^+)$	A	N1	0.2	–4.7	–6.2	10.9
		N2	3.7	–10.4	–11.1	21.5
		H	–1.4	–2.9	–1.7	4.6
	B	N1	7.1	–8.2	–8.7	17.0
		N2	7.1	–8.3	–8.7	17.0
		H	0.2	–2.6	–1.1	3.7
$\text{N}_2^-/\text{MgO}_{\text{Step}}(\text{H}^+)$	L	N1	0.2	–6.3	–4.5	10.8
		N2	4.1	–11.2	–10.4	21.5
		H	–0.4	–1.9	–1.1	3.1
	U	N1	3.6	–8.5	–8.4	16.8
		N2	8.3	–6.3	–5.5	11.8
		H	–0.7	–1.8	–1.1	2.9
$\text{N}_2^-/\text{MgO}_{\text{Corner}}(\text{H}^+)$		N1	5.5	–8.0	–7.5	15.5
		N2	5.5	–8.0	–7.5	15.5
		H	–0.3	–1.1	–0.6	1.7
N_2^-/MgO , exp. ^b		N	4.8	–7.7	–9.0	16.7
		H	–0.1	–0.6	–0.6	1.2

^a From Ref. [23].

^b From Ref. [22].

N_2 gas. The experimental situation in this case is, however, more complicated. In fact, N_2 absorption does not result in a full bleaching as such but only leads to a change in the color of the sample from deep blue to pale blue [19]. This has been attributed to the meta-stability of the $\text{N}_2^-/\text{MgO}(\text{H}^+)$ complexes and to the fact that not all color centers

react with the N_2 molecule, at variance with O_2 . An additional consideration, based on the difference in optical absorption properties of $\text{O}_2^-/\text{MgO}(\text{H}^+)$ and $\text{N}_2^-/\text{MgO}(\text{H}^+)$ centers, is discussed below.

The excitation energies of $\text{O}_2^-/\text{MgO}(\text{H}^+)$ and $\text{N}_2^-/\text{MgO}(\text{H}^+)$ have been calculated using the

time-dependent density functional theory (TD-DFT) approach as implemented in Gaussian98 code. These calculations have demonstrated that the excitation energies and the nature of the transitions are very similar for different $\text{MgO}(\text{H}^+)(\text{e}^-)$ sites. We therefore describe these results for a corner site (see Fig. 4) only.

In the case of the O_2 adsorbed at the $\text{MgO}_{\text{Corner}}(\text{H}^+)(\text{e}^-)$ the first excited state is due to an internal O_2^- transition with the excitation energy of about 0.5 eV. The energy of this transition is almost independent of the adsorption site. The second lowest transition corresponds to the charge transfer from the O_2^- to the four-coordinated cation at the 100 edge site opposite to the adsorption site of O_2^- molecule. This transition is clearly correlated with the local atomic structure of the $\text{O}_2^-/\text{MgO}(\text{H}^+)$ center. In our calculations the energy of this transition was 3.1–3.5 eV depending on the MgO site. We note that both transitions are outside the visible range and have very small, practically zero, transition matrix element. This picture agrees well with the experimental observations of the complete bleaching of the surface color centers in the oxygen atmosphere.

In the case of $\text{N}_2^-/\text{MgO}_{\text{Corner}}(\text{H}^+)$ center, the nature of the optical transitions is similar but the energies are rather different. The first excited state corresponds to intra-molecular transition of N_2^- with the excitation energy of 0.6–0.7 eV. A few following transitions are due to the electron transfer from the N_2^- to the states at the bottom of the conduction band (CB) formed by the nearest and second nearest cation neighbors. In the case of the corner site the bottom of the CB is formed by the four-coordinated cations at the [1 0 0] edge sites and, at higher energies, by five-coordinated cations at terrace sites and the corresponding excitation energies are 1.0, 1.9, and 2.0 eV. Depending on the adsorption site, the transition energies for the $\text{N}_2^- \rightarrow \text{CB}$ absorption are in the range of 1.0–2.9 eV and the corresponding transition matrix elements could be only 3–5 times smaller than those for the color centers. Thus, the exposure of the MgO enriched with color centers to the N_2 gas is expected to only modify the optical absorption but not to remove it completely. This has been indeed observed in the experiment.

4. Conclusions

We have considered the chemical interaction of O_2 and N_2 molecules with electrons trapped at the surface of MgO. Experimentally, it is known that polycrystalline MgO where color centers have been created by chemical methods react instantaneously at low temperature with O_2 and N_2 leading to a complete change in the EPR spectra and to the complete or partial disappearance of the color of the sample. This is considered as a direct proof of the fact that the color centers are located at the surface of the material. The analysis of the EPR spectra shows that the color change is associated with a charge transfer of the trapped electron to the adsorbed molecule and thus, transformation of $\text{MgO}(\text{H}^+)(\text{e}^-)$ into $\text{X}_2^-/\text{MgO}(\text{H}^+)$ centers with different optical absorption spectra. The difference between O_2 and N_2 is that while the first species is stable, N_2 gives rise to a metastable N_2^- anion, which can reversibly transform into N_2 and a trapped electron by moderate thermal treatment.

Any atomistic model of the paramagnetic color centers at the surface of MgO must be able to explain this reactivity. So far, the generally accepted model of color centers on MgO has been that of oxygen vacancies with one trapped electron, F_S^+ . Recently, a new model which better accounts for the general observations and mechanism of generation of surface color centers has been proposed [6,7]. It consists of neutral morphological sites at the MgO surface, which are able to bind a $(\text{H}^+)(\text{e}^-)$ pair. These centers have observable properties (optical transitions, hyperfine constants, vibrations, stability, etc.), which fit very nicely with what is known about paramagnetic color centers on polycrystalline MgO. One aspect, which has not been investigated so far, is the reactivity of these centers towards O_2 and N_2 .

In this study we have considered the reactivity of three members of the family of morphological color centers, the reverse corner, $\text{MgO}_{\text{RC}}(\text{H}^+)(\text{e}^-)$, the step, $\text{MgO}_{\text{Step}}(\text{H}^+)(\text{e}^-)$, and the oxygen terminated corner, $\text{MgO}_{\text{Corner}}(\text{H}^+)(\text{e}^-)$, towards O_2 and N_2 . We confirmed the chemisorption of the O_2 and a metastable character of the N_2 adsorption at

these surface color centers. Moreover, while $\text{O}_2^-/\text{MgO}(\text{H}^+)$ centers have no optical absorption in the visible range, $\text{N}_2^-/\text{MgO}(\text{H}^+)$ absorb weakly and therefore are expected to provide a slight additional coloring of the samples.

The results perfectly fit into the whole picture, providing further support for the new model of electron traps at the MgO surface. The surface sites considered in this paper are only few of a larger variety of possible morphological trapping sites at the MgO surface. Other traps can exist which combine features of the above sites or have an entirely different structure. However, we believe that the results of our calculations remain valid for this wider class of surface traps as well. Further work is planned to confirm this belief.

Acknowledgements

This work has been supported by the “Italian INFN” through the PRA project ISADORA. We thank E. Giamello and M. Chiesa for several useful discussions.

References

- [1] E. Giamello, M.C. Paganini, D. Murphy, A.M. Ferrari, G. Pacchioni, *J. Phys. Chem.* 101 (1997) 971.
- [2] M.C. Paganini, M. Chiesa, E. Giamello, S. Coluccia, G. Martra, D. Murphy, G. Pacchioni, *Surf. Sci.* 421 (1999) 246.
- [3] G. Pacchioni, P. Pescarmona, *Surf. Sci.* 412/413 (1998) 657.
- [4] L. Ojamäe, C. Pisani, *J. Chem. Phys.* 109 (1998) 10984.
- [5] D. Ricci, G. Pacchioni, P.V. Sushko, A.L. Shluger, *J. Chem. Phys.* 117 (2002) 2844.
- [6] D. Ricci, C. Di Valentin, G. Pacchioni, P.V. Sushko, A.L. Shluger, E. Giamello, *J. Am. Chem. Soc.* 125 (2003) 738.
- [7] M. Chiesa, M.C. Paganini, E. Giamello, C. Di Valentin, G. Pacchioni, *Angew. Chem.* 42 (2003) 1759.
- [8] G. Pacchioni, in: *Oxide Surfaces, The Chemical Physics of Solid Surfaces*, vol. 9, Elsevier, Amsterdam, 2001, p. 94.
- [9] R. Wichtendahl, M. Rodriguez-Rodrigo, U. Härtel, H. Kühlenbeck, H.J. Freund, *Surf. Sci.* 423 (1999) 90.
- [10] G. Pacchioni, A.M. Ferrari, E. Giamello, *Chem. Phys. Lett.* 255 (1996) 58.
- [11] M. Sterrer, O. Diwald, E. Knözinger, *J. Phys. Chem. B* 104 (2000) 3601.
- [12] M. Sterrer, O. Diwald, E. Knözinger, P.V. Sushko, A.L. Shluger, *J. Phys. Chem. B* 106 (2002) 12478.
- [13] E. Giamello, A. Ferrero, S. Coluccia, A. Zecchina, *J. Phys. Chem.* 95 (1991) 9385.
- [14] E. Giamello, D. Murphy, L. Ravera, S. Coluccia, A. Zecchina, *J. Chem. Soc. Faraday Trans.* 90 (1994) 3167.
- [15] D. Murphy, E. Giamello, *J. Phys. Chem.* 99 (1995) 15172.
- [16] D. Murphy, R.D. Farley, I.J. Purnell, C. Rowlands, A.R. Jacob, M.C. Paganini, E. Giamello, *J. Phys. Chem. B* 103 (1999) 1944.
- [17] M. Chiesa, E. Giamello, D. Murphy, G. Pacchioni, M.C. Paganini, R. Soave, Z. Sojka, *J. Phys. Chem. B* 105 (2001) 497.
- [18] A.M. Ferrari, G. Pacchioni, *J. Chem. Phys.* 107 (1997) 2066.
- [19] E. Giamello, M.C. Paganini, M. Chiesa, D.M. Murphy, G. Pacchioni, R. Soave, A. Rockenbauer, *J. Phys. Chem. B* 104 (2000) 1887.
- [20] R. Soave, A.M. Ferrari, G. Pacchioni, *J. Phys. Chem.* 105 (2001) 9798.
- [21] A.M. Ferrari, R. Soave, A. D’Ercole, C. Pisani, E. Giamello, G. Pacchioni, *Surf. Sci.* 479 (2001) 83.
- [22] Z. Sojka, M. Chiesa, M.C. Paganini, E. Giamello, *Stud. Surf. Sci. Catal.* 140 (2001) 413.
- [23] M. Chiesa, E. Giamello, M.C. Paganini, Z. Sojka, D. Murphy, *J. Chem. Phys.* 116 (2002) 4266.
- [24] A.J. Tench, R.L. Nelson, *J. Colloid Interface Sci.* 26 (1968) 364.
- [25] A.J. Tench, *Surf. Sci.* 25 (1971) 625.
- [26] J.E. Wertz, P. Auzins, R.A. Weeks, R.H. Silsbee, *Phys. Rev.* 107 (1957) 1535.
- [27] L.A. Kappers, R.L. Kroes, E.B. Hensley, *Phys. Rev. B* 10 (1970) 4151.
- [28] G. Pinarello, C. Pisani, A. D’Ercole, M. Chiesa, M.C. Paganini, E. Giamello, O. Diwald, *Surf. Sci.* 494 (2001) 95.
- [29] P.V. Sushko, J.L. Gavartin, A.L. Shluger, *J. Phys. Chem. B* 106 (2002) 2269.
- [30] S. Brazzelli, C. Di Valentin, G. Pacchioni, M. Chiesa, E. Giamello, *J. Phys. Chem. B*, in press.
- [31] P.V. Sushko, A.L. Shluger, R.C. Baetzold, C.R.A. Catlow, *J. Phys.: Condens. Matter* 12 (2000) 8257.
- [32] W. Stevens, H. Bach, J. Krauss, *J. Chem. Phys.* 81 (1984) 6026.
- [33] P.V. Susko, A.L. Shluger, C.R.A. Catlow, *Surf. Sci.* 450 (2000) 153.
- [34] M.J. Frisch et al., *Gaussian 98, Revision A.6*, Gaussian Inc., Pittsburgh PA, 1998.
- [35] J.E. Dennis, R. Sabel, *Numerical Methods for Unconstrained Optimization and Nonlinear Equations*, Prentice-Hall, Englewood Cliffs, NJ, 1983.
- [36] A.D. Becke, *J. Chem. Phys.* 98 (1993) 5648.
- [37] C. Lee, W. Yang, R.G. Parr, *Phys. Rev. B* 37 (1988) 785.
- [38] M.M. Francl, W.J. Pietro, W.J. Hehre, J.S. Binkley, M.S. Gordon, D.J. De Fries, J.A. Pople, *J. Chem. Phys.* 77 (1982) 3564.
- [39] W.J. Hehre, R. Ditchfield, J.A. Pople, *J. Chem. Phys.* 56 (1972) 2257.
- [40] R. Krishnan, J.S. Binkley, R. Seeger, J.A. Pople, *J. Chem. Phys.* 72 (1980) 650.

- [41] G.L. Gutsev, P.B. Rozyczko, R.J. Bartlett, *J. Chem. Phys.* 110 (1999) 5137.
- [42] CRC Handbook of Chemistry and Physics, CRC Press, Boca Raton, FL, 1994.
- [43] S.F. Boys, F. Bernardi, *Mol. Phys.* 19 (1970) 553.
- [44] J.A. Weil, J.R. Bolton, J.E. Wertz, *Electron Paramagnetic Resonance*, John Wiley & Sons, New York, 1994.